A new mechanism of upwelling generated filaments based on potential vorticity balance

C. Troupin[1], E. Mason[2], J.-M. Beckers[1] & P. Sangrà[2]

[1] Université de Liège, GeoHydrodynamics and Environment Research, Sart-Tilman B5, Liège 1, BELGIUM
[2] Facultad de Ciencias del Mar, Universidad de Las Palmas de Gran Canaria, 35017 Las Palmas de Gran Canaria, SPAIN

1 Abstract

Upwelling filaments are typical features in eastern boundary upwelling systems. Although they are known to enhance primary production in open ocean, physical processes that generate it are not yet perfectly understood.
For this reason we strive to develop a simple theory based on the concept of **potential vorticity conservation**: we assume that **filaments** are **generated by an injection of positive vorticity** near the capes, which impedes the upwelling jet to continue its way southward.
In order to assess the role of possible sources of vorticity, several experiments with the model ROMS are designed and the behavior of the Cape Ghir filament is examined in these different configurations.

2 Description

Upwelling filaments are elongated structures which extent offshore, transporting cold coastal water into the ocean interior. They are clearly identifiable with satellite imagery through their SST signature (Fig.1). Table 1 summarizes filament typical scales.

FIGURE 1: *AVHRR Sea Surface Temperature from 7 to 11 September 2007. Several filaments are visible along the NW Africa coast.*

Table 1: Filament typical scales off African and Iberian coasts, according to García-Munõz et al. (2005), Kostianoy and Zatsepin (1996), Pelegrí et al. (2005), Peliz et al. (2002)

Scale	Units	Value
Length	km	100-250
Width	km	10-75
Depth	m	100-150
Time of activity	days	3-10
ΔT	$°C$	1-2.5

3 Theory

The base hypothesis is the conservation of potential vorticity (PV), defined as

$$PV = \frac{(\boldsymbol{\nabla} \times \mathbf{u}) + f\mathbf{k}}{\rho_0} \cdot \boldsymbol{\nabla}\rho, \qquad (1)$$

where $\mathbf{u}$ is the velocity vector, f the Coriolis parameter, ρ the water density and ρ_0 the reference density.
Numerical experiences will assess the role of different factors able to influence PV (*e.g.* Marshall and Tansley (2001), Signell and Geyer (1991), Thomas (2005)): 1. wind: intensity, direction, curl; 2. topography: bottom, coastline, friction; 3. Coriolis frequency.

4 Model

The ROMS model [Shchepetkin and McWilliams (2003,2005)] is implemented around Cape Ghir (NW Africa, see Fig.2). The method is the following:

1. A reference configuration using realistic atmospheric forcing and bathymetry is implemented, yielding us reasonable physical characteristics for the filament.
2. Modified-condition experiments are run and compared with the reference configurations.
3. Diagnostics are computed for each case and discussed in the frame of our generation hypothesis.

4.1 Configuration

Initial and boundary conditions are extracted from a large-scale solution (domain D1, Fig.2) in the North Atlantic [Mason et al. (a), in prep.] using tool `roms2roms` [Mason et al. (b), in prep.]. Initial and boundary condition for large scale solution are extracted from a high-resolution climatology of the NE Atlantic [Troupin et al., in prep.]. For all domains, atmospheric forcing is interpolated from COADS05 0.5°-resolution fields and wind stress is extracted from Scatterometer Climatology of Ocean Winds (SCOW, Risien and Chelton (2008)) with a resolution of 0.25°. Topography is taken from GEBCO 1−minute global bathymetry.

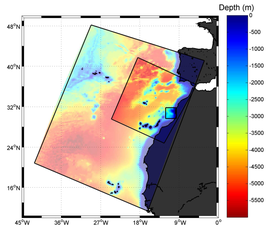

FIGURE 2: *Domains and topography used in the experiments: intermediate (D_2) and small domains have 4 km and 1.5 km resolutions, respectively. Cape Ghir location is indicated by a white dot.*

5 Results

5.1 Generation of filaments

The model configuration was suitable for generating filament with plausible physical characteristics (Fig.3). On the intermediate domain, an upwelling filament extends offshore close to $12°W$ with a temperature difference of about $2°C$ with respect to surrounding waters. On the small domain, the filament is present at the same location, but the trajectory is slightly different: near $11°W$, it turns northward and reaches $31°30'N$.

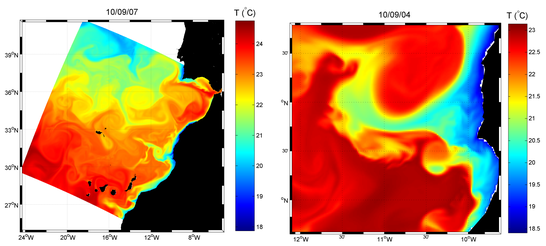

(a) (b)

FIGURE 3: *Surface temperature fields for domains D_2 (a) and D_3 (b) on the 10th of September. Both cases show a filament off Cape Ghir.*

Figure 4 shows that the coastal upwelling is characterized by a zone of lower positive potential vorticity. This allows the flow to travel southward. In the ocean interior, PV decrease from north to south, because of the planetary vorticity.

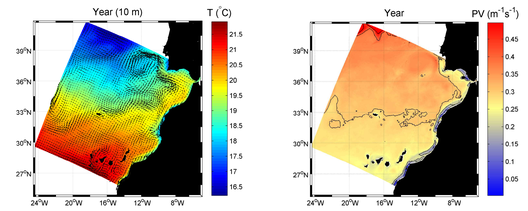

(a) (b)

FIGURE 4: *Annual mean of temperature and potential vorticity at 10 m in domains D_2 (a) and D_3 (b).*

5.2 Reference configuration

September averaged fields for the reference configuration are showed in Fig.5. As the filament position is not exactly the same all the time, its temperature signature does not appear so localized in the figure. A band of negative vorticity is still visible close to the coast.

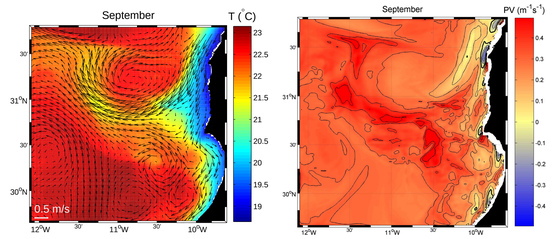

(a) (b)

FIGURE 5: *Temperature and potential vorticity at 10 m in September for the reference configuration.*

5.3 Influence of β-effect

Following our hypothesis, the injection of positive vorticity near the cape makes that the filament is associated to a larger PV, hence it has to turn offshore to conserve its PV. When assuming a constant Coriolis parameter f over D_3 (Fig.6), the filament is not generated: the equatorward decrease of planetary vorticity is not applied anymore, thus the flow is not restricted to go southward. This agrees with Marshall and Tansley (2001), who state that in Eastern Boundary Current (EBC), β-effect enhances the separation of boundary current.

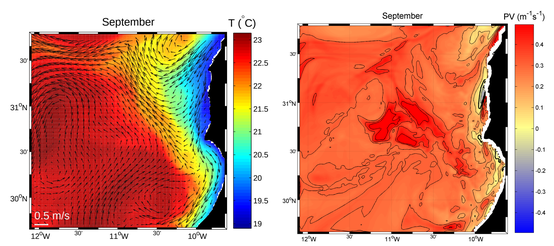

(a) (b)

FIGURE 6: *Temperature and potential vorticity at 10 m in September without β-effect.*

5.4 Wind effect

In order to analyze the effect of wind curl, the model is run with a uniform wind over the whole domain D_3, so that the wind curl is null everywhere. Corresponding results (Fig.7) suggest that without wind contribution, vorticity injection near the cape is not sufficient to induce the detachment of the flow. Castelao and Barth (2007) showed that an increased magnitude of wind curl provokes an earlier establishment of the offshore jet.

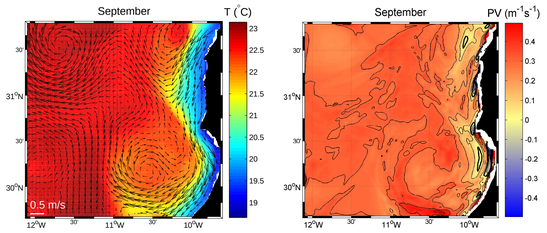

(a) (b)

FIGURE 7: *Temperature and potential vorticity at 10 m in September with uniform wind.*

5.5 Bathymetry effect

When encountering Cape Ghir Plateau (north of Cape Ghir), the southward flow tends to travel over decreasing depths, *i.e.* $\mathbf{u} \cdot \boldsymbol{\nabla} h < 0$. Lee et al. (2001) and Marshall and Tansley (2001) demonstrate that the previous condition is unfavorable to jet separation,
Using a smoothed or a flat bathymetry (Fig.8) has the effect of decreasing the slope $\boldsymbol{\nabla} h$, thus reducing the negative effect the filament formation. This may explain why a filament is generated further north, near $31°30'N$.

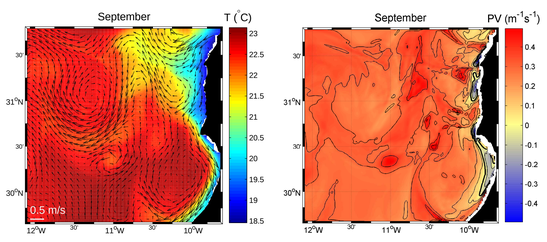

(a) (b)

FIGURE 8: *Temperature and potential vorticity at 10 m in September with the smooth bottom case.*

6 Conclusions

With idealized experiments, the mechanisms for filament generation were studied. Potential vorticity conservation permits to give a simple explanation of the phenomenon. Results suggest that wind vorticiy is the main source of positive vorticity near the Cape Ghir, while bathymetry (*i.e.* Cape Ghir Plateau) is also responsible for an enhancement of the offshore filament.

Acknowledgments

This work was facilitated by a Subside Fédéral pour la Recherche (Belgium) and a travel grant from the Communauté Française de Belgique. The support from the Fonds pour la Formation à la Recherche dans l'Industrie et dans l'Agriculture (FRIA) is greatly appreciated, as well as contributions from the Spanish MEC through the CAIBEX Project.